Structural Virology Hot Paper

International Edition: DOI: 10.1002/anie.201505672
German Edition: DOI: 10.1002/ange.201505672

Attachment of Norovirus to Histo Blood Group Antigens: A Cooperative Multistep Process

*Alvaro Mallagaray, Julia Lockhauserbäumer, Grant Hansman, Charlotte Uetrecht, and Thomas Peters**

Abstract: *Human noroviruses recognize histo blood group antigens (HBGAs) as cellular attachment factors. Recently, it has been discovered that norovirus infection can be significantly enhanced by HBGA binding. Yet the attachment process and how it promotes host-cell entry is only poorly understood. The binding of a norovirus protruding (P) domain of a predominant GII.4 Saga strain to HBGAs at atomic resolution was studied. So far, independent and equivalent multiple binding sites were held responsible for attachment. Using NMR experiments we show that norovirus-HBGA binding is a cooperative multi-step process, and native mass spectrometry reveals four instead of two HBGA binding sites per P-dimer. An accompanying crystallographic study has disclosed four instead of two* L*-fucose binding sites per P-dimer of a related GII.10 strain[1] further supporting our findings. We have uncovered a novel paradigm for norovirus-HBGA recognition that will inspire further studies into norovirus–host interactions.*

The first step of norovirus infection requires attachment of virus particles to histo blood group antigens (HBGAs).[2] To date it is still unknown which cells are infected by noroviruses. A recent study suggested that noroviruses target B-cells after passage of the epithelial monolayer in the duodenum and that infection is facilitated by the presence of enteric bacteria carrying blood group antigens.[3] In parallel, high-resolution structural data from crystal structure analysis of complexes of norovirus coat proteins with HBGAs are becoming more and more available. The viral coat of human noroviruses consists of 180 copies of a single coat protein VP1. Binding to HBGAs requires VP1 dimerization, and the current understanding is that two binding sites exist for each dimer. Truncated dimers, so-called P-dimers, have proven excellent models for in vitro binding studies. Crystal structure analyses have shown that P-dimers are highly symmetrical suggesting equivalent and independent binding sites.[4] Therefore, binding isotherms from ligand titration experiments should follow a simple one-site binding model. Here, we have studied binding of a variety of carbohydrate ligands to P-dimers of a GII.4 human norovirus strain (Saga) using STD NMR[5] titration experiments. In a complementary approach we have subjected uniformly ^{2}H,^{15}N-labeled P-dimers to a chemical shift titration with methyl α-L-fucopyranoside using ^{1}H,^{15}N-TROSY-HSQC experiments[6] as a readout. Finally, we have studied the binding stoichiometry using native mass spectrometry.[7]

For the NMR binding studies we have employed methyl α-L-fucopyranoside **1**, citrate **3**, blood group H-disaccharide **4**, blood group B trisaccharide **5**, Lewis^{x} trisaccharide **7**, and Lewis^{y} tetrasaccharide **8** as ligands, and D-galactose **2** as a negative control (Scheme 1).

For STD NMR experiments expression of P-dimers in *E. coli* essentially followed established protocols.[8] For protein NMR experiments, uniformly ^{2}H,^{15}N-labeled P-dimers

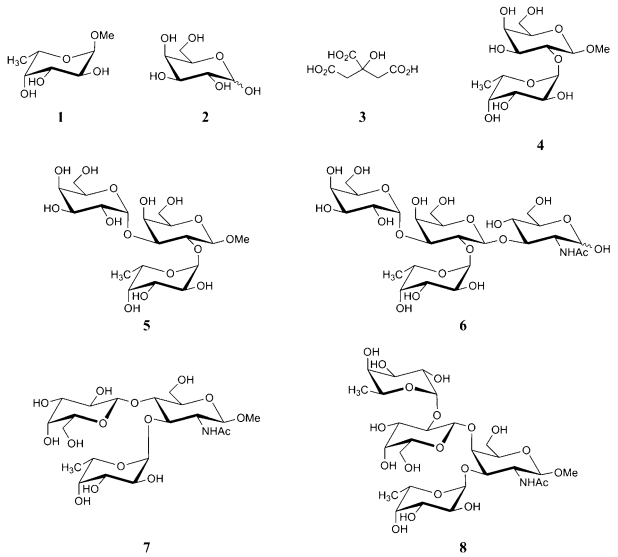

Scheme 1. Carbohydrate structures studied in this work. Methyl α-L-fucopyranoside **1**, D-galactose **2**, citric acid **3**, blood group H-disaccharide **4**, blood group B trisaccharide **5**, type-1 blood group B tetrasaccharide **6**, Lewis^{x} trisaccharide **7**, and Lewis^{y} tetrasaccharide **8**.

[*] Dr. A. Mallagaray, Prof. Dr. T. Peters
Center of Structural and Cell Biology in Medicine
Institute of Chemistry, University of Lübeck
Ratzeburger Allee 160, 23562 Lübeck (Germany)
E-mail: thomas.peters@chemie.uni-luebeck.de
J. Lockhauserbäumer, Dr. C. Uetrecht
Dynamics of Viral Structures, Heinrich Pette Institute
Leibniz Institute for Experimental Virology
Martinistrasse 52, 20251 Hamburg (Germany)
and
Sample Environment Group, European XFEL GmbH
Notkestrasse 85, 22607 Hamburg (Germany)
Dr. G. Hansman
Schaller Research Group at the
University of Heidelberg and the DKFZ
69120 Heidelberg (Germany)
and
Department of Infectious Diseases and Virology
University of Heidelberg, 69120 Heidelberg (Germany)

Supporting information for this article, including experimental details, is available on the WWW under http://dx.doi.org/10.1002/anie.201505672.

were required. Therefore, we have optimized expression of P-dimers in minimal media[9] yielding uniformly ^{2}H,^{15}N-labeled P-dimers in excellent yields. In a first set of experiments we have determined the degree of dimerization of the P-dimers under investigation. Dimerization is a known prerequisite for binding to HBGAs.[10] It is also known that depending on amino acid sequence and lengths of constructs P-dimer preparations may contain varying amounts of monomers. As described in the Supporting Information, P-dimers used in this study exist exclusively in the dimeric state.

STD NMR titration experiments allow determination of dissociation constants K_D for ligand molecules binding to receptor proteins in solution without immobilizing or modifying ligands or receptor proteins.[11] In a direct titration, intensities of STD NMR signals are monitored as a function of the concentration of ligand. Here, methyl α-L-fucopyranoside **1**, blood group H-disaccharide **4**, and blood group B trisaccharide **5** were used as ligands representing the critical binding epitope of HBGAs for GII.4 strains. Citrate **3** was also employed as ligand as it has been shown before to act as a mimic of L-fucose.[12] Typical STD NMR titration curves are shown in Figure 1.

It is obvious that the curves cannot be explained assuming independent and equivalent binding sites.[13] In such a case resulting binding isotherms would be smooth without any steps under all possible conditions. Instead, all binding curves start out as one-site binding isotherms but when a first plateau of saturation is approached successive binding events appear resulting in two or more steps in the titration curve, depending on the ligand. Increasing the concentration of ligands finally leads to saturation, which verifies specific binding. For methyl α-L-fucopyranoside **1** and H-disaccharide **4** we could not increase the ligand concentration above 20 mM because direct irradiation of the ligand occurred. It is observed that the shapes of the curves and the position of the onset of the successive binding events depend on pH, buffer and affinity associated with the primary binding event (Supporting Information, Figure S2). Steps in the binding isotherms reflect binding events with cooperativity.[14] Therefore, we have used a model that superimposes one-site binding as a primary binding event with subsequent cooperative binding steps as described in the materials and methods section (Supporting Information). Non-linear least squares fitting of Equation (1) to the titration data yielded up to four K_D values (K_{D1} to K_{D4}) for each ligand, depending on the number of binding steps n observed:

$$O = \frac{[L]}{K_{D1}+[L]} \bullet O_{max,1} + \sum_{i=2}^{n} \frac{[L]^{h_i}}{(K_{Di})^{h_i}+[L]^{h_i}} \bullet O_{max,i} \qquad (1)$$

with O being the observed parameter changing upon titration, K_{Di} being the microscopic dissociation constants for each binding event, O_{max} being the maximum change of the observable, n being the number of distinct binding steps, and h_i being the Hill coefficient. Here, O is the STD amplification factor ($STD\ AF$) observed at a given free ligand concentration $[L]$.

K_{D1} reflects an initial one-site binding process, and the dissociation constants K_{Di} with $i>1$ report on successive cooperative binding events. We have obtained dissociation constants K_{Di} for methyl α-L-fucopyranoside **1**, citrate **3**, blood group H-disaccharide **4**, and blood group B trisaccharide **5** (Table 1).

The dissociation constants K_{D1} are similar to dissociation constants reported previously for related systems[15] (Table 1). From STD NMR it is clear that increasing the concentration of ligands leads to successive binding events, characterized by additional dissociation constants K_{Di} and associated with cooperativity. In the case of methyl α-L-fucopyranoside **1** and H-disaccharide **4,** two dissociation constants were obtained. Data for further titration points were not acquired because of difficulties with direct irradiation at these higher ligand concentrations. For citrate **3,** no direct irradiation problems were experienced, even at concentrations above 50 mM. Also, the first dissociation constant K_{D1} for citrate is lower than for methyl α-L-fucopyranoside **1** or H-disaccharide **4** shifting the whole titration curve to lower concentrations. Therefore, for citrate **3,** three binding events are observed as this is clearly seen in Figure 1. For blood group B-trisaccharide **5,** a significantly lower K_{D1} value of 60 μM is observed, and in total four binding steps are observed resulting in four respective dissociation constants (Table 1).

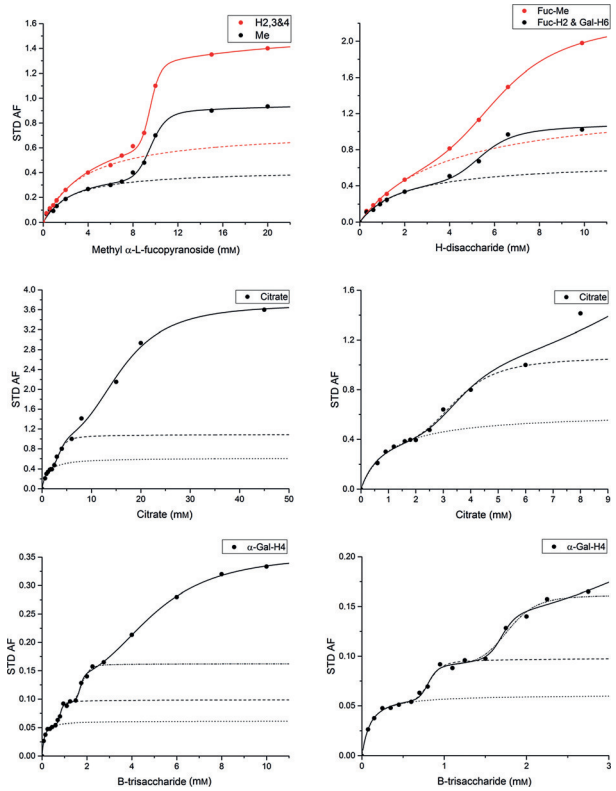

Figure 1. STD NMR titration curves for methyl α-L-fucopyranoside **1** and blood group H-disaccharide **4** (first row), citric acid **3** (second row), and blood group B trisaccharide **5** (third row). The concentration of P-dimers was 30 μM in all cases. The STD amplification factor[11] is shown as a function of ligand concentration. Solid lines result from fitting Eq. (1) to the experimental data. Dashed lines indicate theoretical curves if binding were restricted to the corresponding number of sites (number of steps in the binding curve).

Table 1: Dissociation constants K_{Di} and Hill coefficients h_i from direct STD NMR titrations with corresponding R^2/χ^2 values.

Ligand	K_{D1} [mM]	K_{D2} [mM]	K_{D3} [mM]	K_{D4} [mM]	h_2[a]	h_3[a]	h_4[a]	R^2	χ^2
1	2.4 ± 0.2	9.6 ± 0.1	–	–	12.9 ± 1.5			0.997	0.00007
4	1.9 ± 0.3	5.5 ± 0.4	–	–	8.0 ± 2.4			0.997	0.00016
3[b]	0.8 ± 0.4	3.6 ± 0.3	15.8 ± 0.5	–	4.9 ± 1.4	3.3 ± 0.3		0.996	0.0011
5[c]	0.06 ± 0.02	0.77 ± 0.03	1.65 ± 0.04	4.8 ± 0.17	12.1 ± 5.8	19.2 ± 9.5	3.2 ± 0.4	0.9985	0.00001

[a] In our empirical model given by Equation (1), Hill coefficients h_i have no simple relation to the binding stoichiometry (Supporting Information). [b], [c] Ligand concentrations [*L*] were corrected applying the law of mass action as described in the materials and methods section of the Supporting Information for the first [b], or the first and the second term [c] in Equation (1).

Direct STD NMR titrations require substantial amounts of ligand. Therefore, we also applied a competitive titration procedure using methyl α-L-fucopyranoside **1** as a reporter ligand to obtain dissociation constants for Lewis^x trisaccharide **7** and Lewis^y tetrasaccharide **8**. To compare, we also subjected H-disaccharide **4** and blood group B trisaccharide **5** to this indirect assay format. The dissociation constants from the competitive assay format for H-disaccharide **4** and B-trisaccharide **5** were similar to the K_{D1} values obtained from direct titration experiments (Table 2). This indirect setup does not easily allow picking up multiple-step binding processes, and at the concentrations of protein and ligands chosen, the K_D values obtained via the Cheng–Prusoff equation[16] dominantly reflect the first binding event (Table 2). It is observed that the affinities of blood group B trisaccharide **5**, Lewis^x trisaccharide **7** and Lewis^y tetrasaccharide **8** are about one order of magnitude better than those of methyl α-L-fucopyranoside **1** or blood group H disaccharide **4**.

Table 2: Dissociation constants K_{D1} from competitive STD NMR titrations.

Ligand	K_{D1} [mM]
4	1.3 ± 0.2
5	0.10 ± 0.02
7	0.11 ± 0.02
8	0.15 ± 0.09

To address the question of whether the successive binding events are associated with a change in binding epitopes, we performed STD NMR experiments at a saturation time of 2 s and qualitatively analyzed the binding epitopes[11] of H-disaccharide **4** and B-trisaccharide **5** at low and at high ligand concentrations (Figure S4). It is found that the resulting binding epitopes for H-disaccharide **4** are virtually identical. Likewise, the fucose residue of B-trisaccharide **5** is always receiving the largest fraction of saturation. In contrast, saturation transfer to the terminal α-D-galactose and to the reducing β-D-galactose units clearly depends on the ligand concentration, suggesting varying contributions from different binding pockets.

To characterize changes of the protein during ligand binding we subjected P-dimers to chemical shift perturbation experiments.[17] These experiments reflect changes of the protein backbone during ligand titrations. Such changes occur through interactions between ligand molecules and amino acids, or as a result of remote conformational changes following binding.Therefore, backbone NH chemical shifts as a function of ligand concentration deliver dissociation constants, and at the same time report on binding site topology as well as on potential allosteric conformational changes. P-dimers have a molecular weight of about 70 kDa, which is very large for protein NMR spectroscopy.[18] Fortunately, the ^{1}H,^{15}N-TROSY-HSQC spectra of uniformly ^{2}H,^{15}N-labeled P-dimers were of excellent quality allowing for chemical shift titration experiments (Figure S5).

To analyze the chemical shift perturbations $\Delta\delta$, we followed individual differences in the ^{1}H and ^{15}N dimensions using concentrations of methyl α-L-fucopyranoside **1** ranging from 0.5 mM to 160 mM. A comparison of STD NMR titration data with chemical shift titration data at concentrations of methyl α-L-fucopyranoside **1** larger than 20 mM is not possible. Inspection of the raw chemical shift perturbation data immediately reveals non-linear paths of chemical shifts as a function of ligand concentration (Figure 2).

To obtain information on the number of binding sites or bound species, and to denoise the dataset we performed a singular value decomposition (SVD) of the raw chemical shift titration data as a first step.[19] SVD analysis of the chemical shift data set is described in the Materials and Methods section and exposes the presence of three spectroscopically distinguishable bound states for the binding of methyl α-L-fucopyranoside **1** to P-dimers (Supporting Information).

A chemical shift matrix was then reconstructed using four non-noise components, yielding a data set that was essentially identical to the raw data set (Supporting Information). This reconstructed data set was used to determine significant chemical shift perturbations $\Delta\delta$ for both dimensions, ^{1}H and ^{15}N. Chemical shift perturbations $\Delta\delta_{1H}$ and $\Delta\delta_{15N}$ were followed as a function of ligand concentration [*L*], and global non-linear least squares fitting of Equation (1) to the titration data delivered dissociation constants K_{Di}. In this case *O* in Equation (1) is the observed chemical shift perturbation in either dimension ($\Delta\delta_{obs}$). The corresponding titration curves are shown in Figure S10. In total, 116 denoised binding curves were globally fitted resulting in three dissociation constants K_{D1}, K_{D2}, and K_{D3} corresponding to the formation of three bound species (Table 3). The values for K_{D1} and K_{D2} are almost identical with those obtained from STD NMR titrations (Tables 1 and 2).

It is instructive to analyze individual chemical shifts as a function of ligand concentration (Figure 2) and corresponding titration curves (Figures S8 and S9). It is apparent that

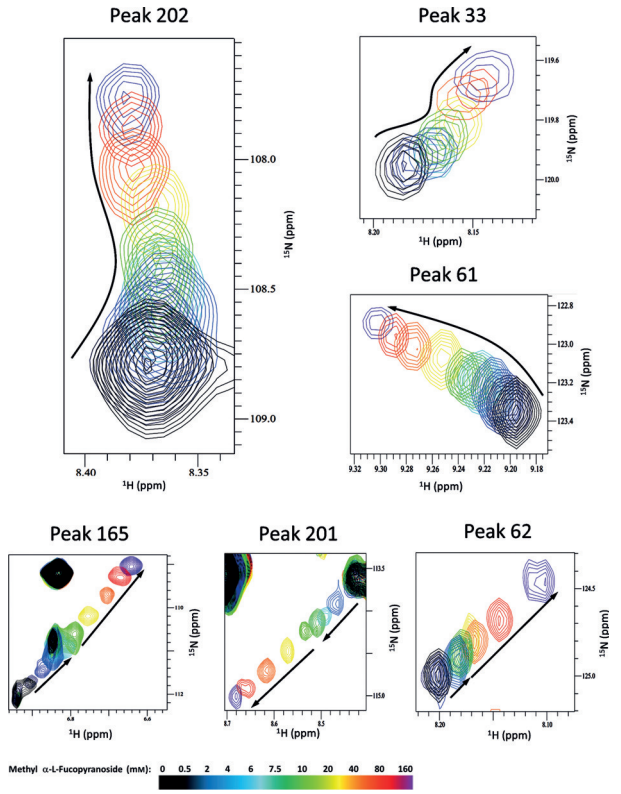

Figure 2. Chemical shifts of individual cross peaks of the ^{1}H,^{15}N-TROSY-HSQC spectra of uniformly ^{2}H,^{15}N labeled GII.4 Saga P-dimers as a function of increasing amounts of methyl α-L-fucopyranoside **1**. Peak numbers correspond to the peaks in the complete spectrum shown in Figure S5.

Table 3: Dissociation constants K_{Di} from chemical shift titrations.

Ligand	K_{D1} [mM]	K_{D2} [mM]	K_{D3} [mM]	R^2/χ^2
1	2.8 ± 0.3	8.9 ± 0.2	36.3 ± 3.1	$0.9992/1.26\times10^{-4}$

many peaks such as peak 202, peak 33, and peak 61 follow non-linear paths during the titration, reflecting multistep binding events (Figure 2). The two largest chemical shift perturbations were observed for peaks 165 and 201, respectively. For peak 165 a distinctive change of direction of the chemical shift is observed at a ligand concentration of ca. 7 mM (Figure 2), which corresponds to a small step in the corresponding titration curve (Figure S9). This ligand concentration corresponds to the value at which the STD NMR titration curve (Figure 1) exhibits a step indicating the presence of a second cooperative binding event. Thus, this titration curve mainly reflects dissociation constants K_{D1} and K_{D2}. For cross-peak 201 the bend at about 7 mM ligand concentration is less pronounced; therefore, the curve mostly reflects binding associated with K_{D2}. Other titration curves reach saturation at ligand concentrations well below 10 mM reflecting exclusively the first binding event. Some peaks show almost no movement during the initial phase of titration, as seen for example in peak 62 (Figure 2). This leads to a sigmoidal shape of the corresponding titration curve (shown for peak 10 in Figure S9). Thus, chemical shift titration curves may emphasize individual steps of the binding process to varying extent depending on the position of the corresponding amino acid, and on how this amino acid is involved in ligand binding.

Native mass spectrometry experiments were performed to directly analyze the binding stoichiometry at different ligand-to-protein ratios.[7b,15] For these experiments we used blood group B type-1 tetrasaccharide **6** as a ligand. Two ligand concentrations of 0.2 mM and 0.5 mM (at a concentration of 2.25 μM of P-dimers) were used employing cytochrome C as a non-binding reference. The result of this study revealed that the higher concentration of B type-1 tetrasaccharide **6** leads to the formation of complexes with one to four ligands bound (Figure 3).

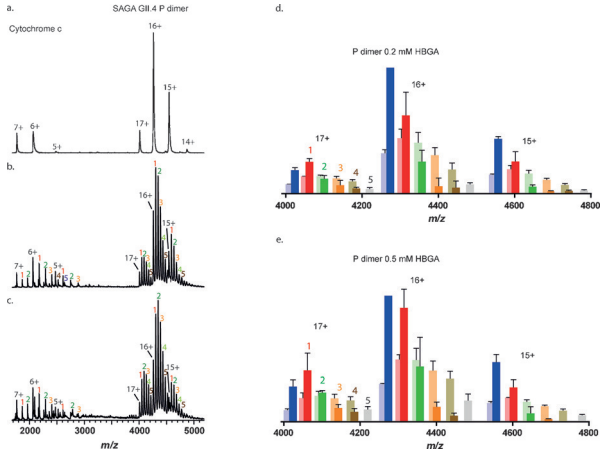

Figure 3. Native mass spectra of B-type 1 tetrasaccharide **6** binding to GII.4 Saga P-dimers. Cytochrome c served as a reference to correct for unspecific binding. It is obvious that up to four ligands bind to the P-dimers. a)–c) Uncorrected spectra at 0, 0.2, and 0.5 mM tetrasaccharide, respectively; d), e) corrected spectra at 0.2 and 0.5 mM tetrasaccharide, respectively. Raw intensities are displayed in pale, specific ligand binding in bright colors. Numbers above peaks indicate number of bound ligands. Charge states for each peak are given. Intensities are normalized to the highest peak.

At a ligand concentration of 0.2 mM, the signals corresponding to three and four bound ligands have the same intensity, which is a strong indication for cooperative binding. This is in perfect agreement with the observation of four cooperatively coupled binding steps as seen in STD NMR titrations with blood group B trisaccharide **5**.

Our findings are in sharp contrast to existing models for the binding of HBGAs to P-dimers. So far, crystallographic studies have revealed two symmetrical binding pockets whereas our data imply the presence of four non-equivalent sites that are occupied in a stepwise and concentration dependent manner. Therefore, we predicted that increasing ligand concentrations would promote binding to hitherto unknown binding pockets, and we performed co-crystallization experiments with increasing concentrations of L-fucose or blood group B trisaccharide **5**. For the GII.4 Saga strain used in the present study, crystallization under these conditions was not successful so far, although at lower ligand

concentrations a number of HBGA ligands had been successfully co-crystallized.[4b] For a related GII.10 (Vietnam 026) strain respective co-crystals were obtained and yielded high quality crystal structures.[1] For L-fucose, two new binding pockets were identified positioned along the cleft that is created by dimerization and that runs between the two known binding sites. This crystallization study also revealed that occupation of L-fucose binding sites occurred in a stepwise and concentration-dependent manner. Interestingly, the known binding sites were also occupied in a stepwise manner, which had not occurred if the binding sites were independent and equal. In fact, crystal structure analysis revealed loop motions in the vicinity to the L-fucose binding pocket that break the symmetry of P-dimers. These data match the results from the chemical shift titrations, where three bound species have been identified for the binding of methyl α-L-fucopyranoside **1** to P-dimers. In the light of the crystallographic data, the first binding event reflects occupation of one of the known binding sites. The second binding event shows cooperativity and reflects occupation of the second known binding site. The third binding event is due to simultaneous binding of two methyl α-L-fucopyranoside molecules **1** to the newly discovered adjacent fucose binding pockets. Inspection of available crystal structures of P-dimers of noroviruses suggests that the cleft running between the known binding sites is always present, and most likely exists in any calicivirus. Finally, using our binding model and dissociation constants from Table 1 for binding of methyl α-L-fucopyranoside **1** to GII.4 P-dimers, we have estimated the occupation of binding pockets as a function of ligand concentration (Figure S11). It is found that our binding model correctly predicts the stepwise occupation of fucose binding pockets as seen by crystallography.

Our study reveals that binding and recognition of HBGAs by noroviruses is much more complex than thought. In particular, successive binding steps are cooperatively coupled, as shown in Figure 4 for blood group B trisaccharide **5**. We suggest that the cooperative nature of virus-HBGA interaction provides a control or selection mechanism for host-cell entry. This has important implications. The most direct impact will be on studies targeting the entry mechanism of noroviruses. As cell culture systems for noroviruses are emerging[3] it will now be of interest to study how stepwise and cooperative binding appears under in vivo conditions and how it affects infectivity. Another aspect concerns the development of entry inhibitors. Clearly, the design of entry inhibitors[20] has to be revisited taking into account the presence of a dense network of cooperatively coupled HBGA binding sites. We speculate that our findings are general for the family of *Caliciviridae*.

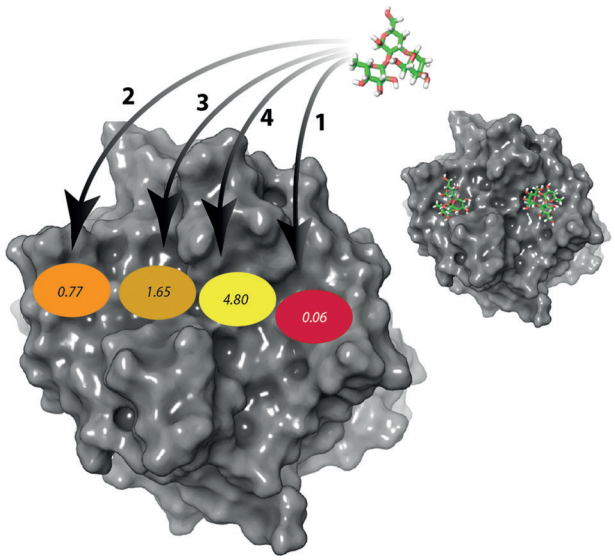

Figure 4. Model for binding of blood group B trisaccharide **5** to GII.4 Saga P-dimers based on crystal structure data[4b] (pdb code: 4X06). Binding occurs in four cooperatively coupled steps as this is reflected by the STD NMR titration curve in Figure 2. Binding to site 1 (red) initially impedes binding to the other sites up to a concentration threshold of ca. 0.5 mM of B trisaccharide **5**. The numbers are the dissociation constants taken from Table 1 in [mM]. The background picture shows occupation of the two known binding sites 1 and 2 as seen in the crystal structure.

Acknowledgements

A.M. is recipient of a Marie Curie fellowship within the 7th Framework Programme of the EU (Grant Agreement No. 329485, NoroCarb). T.P. acknowledges continuing support by the University of Lubeck. J.L. is part of the DELIGRAH graduate school funded by the federal state of Hamburg and C.U. is supported by an SAW-2014-HPI-4 grant from the Leibniz association. Hao Yan is thanked for his contributions to the initial experimental setup. The authors are grateful to Dr. Hanne Peters for generating the conditions under which protein expression and stable isotope labeling became successful.

Keywords: carbohydrates · cooperative binding · multivalency · native mass spectrometry · NMR spectroscopy

How to cite: *Angew. Chem. Int. Ed.* **2015**, *54*, 12014–12019
Angew. Chem. **2015**, *127*, 12182–12187

[1] A. D. Koromyslova, M. M. Leuthold, M. W. Bowler, G. S. Hansman, *Virology* **2015**, *483*, 203–208.
[2] a) P. R. Harrington, L. Lindesmith, B. Yount, C. L. Moe, R. S. Baric, *J. Virol.* **2002**, *76*, 12335–12343; b) A. M. Hutson, R. L. Atmar, D. Y. Graham, M. K. Estes, *J. Infect. Dis.* **2002**, *185*, 1335–1337; c) L. Lindesmith, C. Moe, S. Marionneau, N. Ruvoen, X. Jiang, L. Lindblad, P. Stewart, J. LePendu, R. Baric, *Nat. Med.* **2003**, *9*, 548–553.
[3] M. K. Jones, M. Watanabe, S. Zhu, C. L. Graves, L. R. Keyes, K. R. Grau, M. B. Gonzalez-Hernandez, N. M. Iovine, C. E. Wobus, J. Vinje, S. A. Tibbetts, S. M. Wallet, S. M. Karst, *Science* **2014**, *346*, 755–759.
[4] a) S. Cao, Z. Lou, M. Tan, Y. Chen, Y. Liu, Z. Zhang, X. C. Zhang, X. Jiang, X. Li, Z. Rao, *J. Virol.* **2007**, *81*, 5949–5957; b) B. K. Singh, M. M. Leuthold, G. S. Hansman, *J. Virol.* **2015**, *89*, 2024–2040.
[5] M. Mayer, B. Meyer, *Angew. Chem. Int. Ed.* **1999**, *38*, 1784–1787; *Angew. Chem.* **1999**, *111*, 1902–1906.
[6] K. Pervushin, R. Riek, G. Wider, K. Wuthrich, *Proc. Natl. Acad. Sci. USA* **1997**, *94*, 12366–12371.
[7] a) C. Uetrecht, A. J. R. Heck, *Angew. Chem. Int. Ed.* **2011**, *50*, 8248–8262; *Angew. Chem.* **2011**, *123*, 8398–8413; b) J. Sun,

E. N. Kitova, W. Wang, J. S. Klassen, *Anal. Chem.* **2006**, *78*, 3010 – 3018.
[8] G. S. Hansman, C. Biertumpfel, I. Georgiev, J. S. McLellan, L. Chen, T. Zhou, K. Katayama, P. D. Kwong, *J. Virol.* **2011**, *85*, 6687 – 6701.
[9] V. Tugarinov, V. Kanelis, L. E. Kay, *Nat. Protoc.* **2006**, *1*, 749 – 754.
[10] M. Tan, R. S. Hegde, X. Jiang, *J. Virol.* **2004**, *78*, 6233 – 6242.
[11] M. Mayer, B. Meyer, *J. Am. Chem. Soc.* **2001**, *123*, 6108 – 6117.
[12] G. S. Hansman, S. Shahzad-Ul-Hussan, J. S. McLellan, G. Y. Chuang, I. Georgiev, T. Shimoike, K. Katayama, C. A. Bewley, P. D. Kwong, *J. Virol.* **2012**, *86*, 284 – 292.
[13] D. E. Koshland, G. Némethy, D. Filmer, *Biochemistry* **1966**, *5*, 365 – 385.
[14] A. Levitzki, D. E. Koshland, *Proc. Natl. Acad. Sci. USA* **1969**, *62*, 1121 – 1128.
[15] L. Han, P. I. Kitov, E. N. Kitova, M. Tan, L. Wang, M. Xia, X. Jiang, J. S. Klassen, *Glycobiology* **2013**, *23*, 276 – 285.
[16] Y. Cheng, W. H. Prusoff, *Biochem. Pharmacol.* **1973**, *22*, 3099 – 3108.
[17] M. P. Williamson, *Prog. Nucl. Magn. Reson. Spectrosc.* **2013**, *73*, 1 – 16.
[18] V. Tugarinov, P. M. Hwang, L. E. Kay, *Annu. Rev. Biochem.* **2004**, *73*, 107 – 146.
[19] M. Arai, J. C. Ferreon, P. E. Wright, *J. Am. Chem. Soc.* **2012**, *134*, 3792 – 3803.
[20] a) C. Rademacher, J. Guiard, P. I. Kitov, B. Fiege, K. P. Dalton, F. Parra, D. R. Bundle, T. Peters, *Chem. Eur. J.* **2011**, *17*, 7442 – 7453; b) J. Guiard, B. Fiege, P. I. Kitov, T. Peters, D. R. Bundle, *Chem. Eur. J.* **2011**, *17*, 7438 – 7441.

Received: June 19, 2015
Published online: August 19, 2015

